Hofmann *et al. Energy Mater.* **2025**, *5*, 500092
DOI: 10.20517/energymater.2024.281

Energy Materials

Article

Open Access

Check for updates

How carboxymethylcellulose adsorption and porous active material particles diminish the adhesion of graphite-silicon anodes in lithium-ion batteries

Katarzyna Hofmann[*], **Norbert Willenbacher**

Karlsruhe Institute of Technology, Institute for Mechanical Process Engineering and Mechanics, Karlsruhe 76131, Germany.

[*]**Correspondence to:** Katarzyna Hofmann, Karlsruhe Institute of Technology, Institute for Mechanical Process Engineering and Mechanics, Gotthard-Franz-Str. 3, Karlsruhe 76131, Germany. E-mail: katarzyna.hofmann@kit.edu

How to cite this article: Hofmann, K.; Willenbacher, N. How carboxymethylcellulose adsorption and porous active material particles diminish the adhesion of graphite-silicon anodes in lithium-ion batteries. *Energy Mater.* **2025**, *5*, 500092. https://dx.doi.org/10.20517/energymater.2024.281

Received: 10 Dec 2024 **First Decision:** 8 Jan 2025 **Revised:** 20 Jan 2025 **Accepted:** 7 Mar 2025 **Published:** 25 Apr 2025

Academic Editor: Hong Xu **Copy Editor:** Ping Zhang **Production Editor:** Ping Zhang

Abstract

Due to its adsorption on graphite and superior thickening properties, carboxymethylcellulose (CMC) is widely used as a dispersant and rheology modifier in water-based anode slurries for lithium-ion batteries. CMC also provides cohesion to the dry anode layer but exhibits poor adhesion to the copper foil necessitating the addition of styrene-butadiene rubber (SBR) as an adhesion promoter. High adhesion between the electrode layer and the current collector is crucial in electrode fabrication, especially for electrodes with higher mass loadings. In this work, we investigate how a polymeric binder, originally intended as a thickening and dispersing agent, can significantly affect the adhesive strength between the anode layer and the current collector. Our results reveal that CMC, by adsorbing onto active material particles (graphite, micro-silicon or nano-silicon), indirectly influences the anode adhesion. The adsorbed CMC layer hinders the direct binding of SBR to the active material particles, thereby creating the weakest link between the active layer and the current collector. This effect is more pronounced the higher the CMC molecular weight. Moreover, we could show that graphite-nano-silicon composite anodes exhibit a significantly reduced adhesion to the copper foil despite a low adsorption of CMC on nano-silicon, since a large fraction of SBR particles are trapped in the porous, micron-sized nano-silicon aggregates. Our findings highlight the importance of considering thickener adsorption on active material particles within electrode design, as a factor that exerts an indirect, albeit significant, influence on anode adhesion.

Keywords: Adhesion, silicon anodes, CMC, SBR, polymeric binders, lithium-ion battery

INTRODUCTION

By the year 2035, more than one in four vehicles is expected to be electric[1]. The leading battery energy storage technology for electric vehicles is currently the lithium-ion battery (LIB)[2]. Although this technology has been described as the key to green transformation, there are still some environmental concerns associated with the use of rare earth metals, energy-intensive production, and unresolved recycling issues. In terms of sustainability and production efficiency improvements, aqueous processing represents the state-of-the-art in anode manufacturing. Using water as a non-toxic solvent is more environmentally friendly, reduces energy consumption during the drying process, and consequently lowers manufacturing costs compared to conventional anodes formulated with organic solvents[3-5].

The most commonly used polymeric binder in water-based anode slurries is sodium carboxymethylcellulose (CMC), an anionic water-soluble polyelectrolyte derived from cellulose. It consists of β-glucopyranose monomers, with some hydroxyl groups replaced by carboxymethyl groups. The average number of substituted hydroxyl groups per glucose unit is defined as the degree of substitution (DS) and typically ranges from 0.6 to 1.2. A higher DS generally improves the water solubility of CMC[6,7]. CMC adsorbs onto graphite and acts as a dispersant, sterically stabilizing the active material particles[8,9]. Due to the superior thickening properties in aqueous solutions, CMC allows modulation of slurry viscosity across a wide range at relatively low concentrations, compared to other binders such as linear polyacrylic acid (PAA). Furthermore, depending on the shape of the active material particles, CMC can promote their alignment in a single direction, thereby enhancing the cohesion of the dry anode layers[10]. However, poor adhesion of CMC to the copper current collector necessitates the addition of a second polymer, most commonly styrene-butadiene rubber (SBR), which acts as an adhesion promoter, thereby ensuring a robust connection between the anode active layer and the current collector.

In an aqueous environment, such as a water-based electrode slurry, polymers may either exist as free chains dissolved in a liquid phase or undergo adsorption onto the surface of dispersed particles. In the case of unbound binders, an unfavorable migration phenomenon may occur during the drying process, resulting in binder segregation[9,11-13], which, in turn, directly affects the mechanical (adhesion and cohesion) and electrochemical properties of electrodes[12].

There are many theories describing the phenomenon of adhesion but the most common are mechanical interlocking, adsorption theory, and chemical bonding mechanisms[14,15]. Mechanical bonding is typical for porous materials and relies on the binder embedding into the pores of the substrate[16]. Furthermore, according to adsorption theory, adhesion occurs due to molecular contact and the resulting van der Waals forces between adhesive molecules and the substrate. Additionally, in some cases, adhesive reacts with the substrate, forming chemical bonds[14].

In our previous study[17], we demonstrated that a stable electrode layer that strongly adheres to the current collector foil and maintains high cohesion between particles plays a vital role in the electrode fabrication process, especially at higher mass loadings. This is because such anodes can withstand the stresses that occur during manufacturing steps such as winding, bending, and cutting or punching. However, the impact of adhesion on electrochemical performance is less significant, as even low adhesion levels are sufficient to maintain mechanical and electrical integrity during cell cycling. Therefore, optimizing a binder system is challenging, as it requires a comprehensive understanding of the interactions between the binder and the particles, as well as between the binders themselves.

In recent years, a significant amount of scientific effort has been dedicated to the development of multifunctional polymeric binders, particularly for silicon anodes[18-21]. These polymers have been shown to facilitate robust connection between active material particles and the current collector, while at the same time providing a flexible bond between the silicon particles. The self-healing properties of these binders enable silicon-containing anodes to withstand substantial volume changes during cycling[14], thereby contributing to their superior electrochemical performance. Xiang *et al.*[22] recently introduced a three-dimensional (3D) AGE binder, synthesized from guar gum (GG), gum arabic (GA) and epichlorohydrin (ECH). The formation of hydrogen bonds between the GG, GA and silicon particles strengthens the bond between the binder and the silicon active material. In addition, the spiderweb-like structure of the binder reinforces the electrode, providing structural stability and preventing degradation during cycling. Meanwhile, alternative approaches, such as multilayer coatings, are being developed to facilitate the production of electrodes with superior mechanical and electrochemical properties[23-25]. This method enhances the effective utilization of polymeric binders, simultaneously enabling a reduction in their content. The present study investigates the combination of commercially available CMC and SBR binders, which, with their distinct functionalities, represent a state-of-the-art binder system for aqueous-processed graphite and silicon-containing anodes.

It has been demonstrated that CMC is incapable of enhancing electrode adhesion. Gordon *et al.*[10] showed that for graphite electrodes with CMC as binder only, the adhesion strength is weak, independent of CMC concentration, DS, and molecular weight (M_w). There are studies in the literature investigating the adsorption behavior of CMC on both graphite[8,26,27] and silicon[28-31] active materials. Several groups have reported a correlation between the amount of CMC adsorbed on active material particles and the adhesion strength of anodes. Kim *et al.*[32] in their investigation into the use of different binders for silicon anode slurries demonstrate that there is an inverse correlation between the polymer adsorption and adhesion strength of anodes prepared with CMC and SBR at pH 7. Haberzettl *et al.*[33] examined the impact of the energy input within the mixing process of silicon-graphite anode slurries. Similarly, it was observed that corresponding electrodes with the highest amount of CMC adsorbed on the active material particles exhibited the lowest adhesion. Nevertheless, neither study attempted to provide an explanation for this phenomenon.

In this work, we elucidate how a polymeric binder, originally intended as a thickening and dispersing agent, can have a significant impact on the strength of electrode adhesion. The main objective of this study is to understand how the adsorption behavior of CMC on active material particles affects the adhesive strength of aqueous-processed LIB anodes. This investigation is conducted for graphite and silicon-graphite electrodes to identify potential formulation improvements, ultimately contributing to more efficient and durable energy storage solutions.

EXPERIMENTAL

Materials

Surface-modified natural graphite (Gr, SMG A5, Showa Denko Materials Co, Ltd., Japan) and two different types of silicon powder: micron-sized crystalline silicon (Silgrain® e-Si 410, Elkem, Norway) and nano-sized polycrystalline silicon (Nanostructured & Amorphous Materials Inc., USA) were used as anode active materials (AMs) in this study [Supplementary Figure 1]. A volume-based average diameter and a Brunauer-Emmett-Teller (BET) surface area are 17.8 µm and 3.0 m^2g^{-1} for graphite, 3.3 µm and 3.2 m^2g^{-1} for micro-silicon, 100 nm and 56.4 m^2g^{-1} for nano-silicon. Carbon black (CB, C-Nergy Super C65, Imerys Graphite & Carbon, Switzerland) with an average primary particle size of 32 nm was used as a conductive additive in anode slurries. Both nano-Si and CB particles in aqueous suspensions tend to form agglomerates

with an average size of approximately 5 μm.

Three polymers were used for the study: sodium CMC (TEXTURECEL, DuPont, USA) with a DS of 0.7 and three different M_w of about 150 kDa, 700 kDa and 1200 kDa, polyethylene oxide (PEO, Sigma Aldrich, Germany) with a M_w of 1000 kDa, and styrene butadiene rubber (SBR) in the form of 48 wt% (TRD 2001, JSR, Japan) aqueous dispersion of nanoparticles.

Sample preparation

SBR adhesion

The adhesion of SBR to four different substrates was examined. For this purpose, a polished graphite plate with the dimensions of 100 × 50 × 10 mm (EXC, Graphite24.com GbR, Germany) and a polished quartz glass plate measuring 139 × 102 × 3 mm (EN08NB, GVB GmbH, Germany) were used as equivalent surfaces for the carbon-based anode components and silicon active material, respectively. Three-dimensional-printed frames (40 × 80 mm) were attached to the substrates using double-sided adhesive tape. Subsequently, SBR suspension was poured in and left to dry at room temperature for at least 14 days. Once the samples were dry, the frames were removed. To suppress the elongation of the polymer film during the peel test, duct tape (4615, tesa SE, Germany) was applied to the SBR surface and the samples were cut to a width of 25 mm. To determine the adhesion between SBR and CMC, SBR suspension was poured onto glass plates with 3D-printed frames (125 × 60 mm) and left to dry at room temperature for approximately 14 days. The dry SBR film was then cut into samples of 29 mm in width and removed from the glass plate. In the next step, a 2.4 wt% CMC solution (700 kDa) was poured onto glass plates with 3D-printed frames (125 × 60 mm) and dried in an oven at 40 °C for approximately three days. Lastly, when the CMC film was only slightly damp, the cut SBR film was positioned on top of the CMC film and weighed down. The sample was then left to dry at room temperature until it was completely dry according to gravimetric verification. Finally, the duct tape was applied to the SBR surface and the sample was then cut to a width of 25 mm. In order to ascertain the adhesive strength between SBR and copper foil, an SBR emulsion was coated with a doctor blade (ZUA 2000, Zehntner GmbH, Switzerland) on a copper foil with a thickness of 10 μm. The coating gap was set at 300 μm resulting in a dry SBR film of about 120 μm thickness. The samples were allowed to dry for approximately four days at room temperature.

CMC adsorption

The CMC powder was dissolved in distilled water by stirring with a propeller at 800 rpm for 30 min to prepare CMC solutions. The particle suspensions were prepared by dispersing an appropriate quantity of AM powder in 0.1 vol% CMC solution. Graphite and micro-Si particles were dispersed using a SpeedMixer (DAC 150.1 FVZ, Hauschild, Germany) at 2000 rpm for 2 min, followed by a further 10 min in an ultrasonic bath (RK106, Bandelin Electronics, Germany). As the nano-Si particles could not be sufficiently dispersed using the aforementioned method, a dissolver stirrer was applied at 1200 rpm for 10 min. The pH of the CMC/particle suspensions was observed to range from 7 to 8. After about 30 min, the samples were centrifuged (Eppendorf 5430, Germany) until a transparent supernatant was obtained. In addition, a blank sample was included for each CMC/particle combination to assess whether the sample preparation, including mixing and centrifugation, influenced the properties of the CMC solution (e.g., potential breaking of polymer chains). Following centrifugation, a transparent supernatant was carefully separated from the sediment and taken for further investigation.

Anode preparation

In the first step, a CMC or PEO solution was prepared by dissolving CMC or PEO powder in 95% of the total amount of distilled water by stirring with a propeller (55 mm in diameter) at 1200 rpm for 30 min. The

final concentrations of CMC and PEO solutions were 1.2 wt% (0.8 vol%) and 2.9 wt% (2.6 vol%), respectively. In the subsequent step, the propeller was replaced with a dissolver (50 mm in diameter) and CB was added to the polymer solution. Subsequently, the mixture was stirred at 2000 rpm for 5 min. In the case of silicon-containing slurries in which 20% of the mass of graphite was replaced with silicon, the silicon was added initially, followed by the graphite. The mixture was then stirred for 5 min for each component. For slurries comprising solely graphite, the graphite powder was stirred for 10 min, thus ensuring uniformity in the total stirring time across all slurries. Subsequently, the SBR suspension was introduced, followed by the addition of the remaining 5% of distilled water and stirred for 5 min each. All slurries had a solids content of 42 wt% (25 vol%). Following the mixing process, the slurries were degassed in a desiccator and coated on a 10 μm thick copper foil (SE-Cu, Schlenk Metallfolien GmbH & Co. KG, Germany) using a doctor blade (ZUA 2000, Zehntner GmbH, Switzerland). The coating velocity was set at 10 mm s^{-1} and the coating gap at 100 μm. Subsequently, the anodes were subjected to a drying process at 70 °C for 30 minutes. The dry electrodes, comprising CMC/SBR, contain 93.5 wt% of active material, 1.9 wt% CB, 1.7 wt% CMC and 2.9 wt% SBR. The dry electrodes comprising PEO consist of 91 wt% active material, 1.9 wt% CB, 4 wt% PEO and 2.8 wt% SBR. The anode thickness after drying was approximately 65 ± 2 μm.

Methods

CMC adsorption

A rheological approach was employed to investigate the adsorption of CMC on three distinct types of active material across a series of volume ratios (R) of AM to CMC (R = 1, 3, 5, 7, 10, 15). The initial CMC concentration was maintained at 0.1 vol% for all suspensions, while the particle amount was varied. Initially, the zero-shear viscosities of CMC solutions with volume concentrations of 0.01 vol%, 0.02 vol%, 0.04 vol%, 0.06 vol%, 0.08 vol%, and 0.10 vol% were determined to establish calibration curves, illustrating the relationship between zero-shear viscosity and CMC concentration for each M_w of CMC. Subsequently, the zero-shear viscosities of the mother CMC solutions used to prepare the polymer-particle suspensions, and CMC solutions after adsorption (supernatants) were determined. This enabled the calculation of corresponding CMC concentrations. By comparing the CMC concentration before and after adsorption, the volume of adsorbed CMC was quantified. The flow curves were measured with a stress-controlled rotational rheometer (Physica, MCR 501, Anton Paar GmbH, Germany) with a concentric cylinder geometry (C-CC27/ T200/SS) in a logarithmic shear rate ramp (10 points per decade) in the range $\dot{\gamma}$ = 1 - 1000 s^{-1} and in a logarithmic time scale t = 30 - 10 s. All measurements were conducted at a constant temperature of 20 °C.

Adhesion

We performed 90°-peel tests to determine the adhesive strength of electrode samples (prepared as described in the section "Anode preparation") and SBR films coated on various substrates (prepared as described in the section "SBR adhesion"). A universal testing machine (Texture Analyser TA.XT plus, Stable Micro Systems, UK) with a load cell of 5 kg (for electrode samples) and 50 kg (for SBR films-substrate samples) was utilized. The specimens were affixed to the movable plate using a double-sided adhesive tape and peeled off at a constant velocity of 5 mm s^{-1}. The recorded force was normalized to the sample width to obtain the line load, which was used as a measure of adhesion. At least ten electrode samples of a single formulation and three SBR-substrate samples for each combination were tested. The measured forces for each set of samples were then averaged, and the resulting mean and the standard deviation were calculated. These latter values were then represented graphically as error bars.

Determination of the amount of SBR residue in Si sediment

Nano-Si and micro-Si powders were added to a dilute SBR emulsion and dispersed in an ultrasonic bath for 15 min. The suspensions with a particle concentration of 1.6 wt% and a silicon-to-SBR mass ratio of 5 were

subjected to centrifugation. The sediment was then washed three times with distilled water and dried at 60 °C until it was completely dry according to gravimetric verification. The same procedure was carried out on silicon suspensions without SBR to estimate the mass of the oxidation layer. The dried sediments were weighed and the percentage of SBR retained in the sediment was calculated.

RESULTS AND DISCUSSION

Adhesion of SBR films to anode components

This section presents an examination of the adhesive strength between SBR films and substrates representing anode components. The results were obtained from 90°-peel tests conducted on samples of bulk materials. For this purpose, a quartz glass plate served as an equivalent surface for the silicon active material, whereas a graphite plate represented the carbon-based anode components, including both graphite and CB.

Figure 1 illustrates that SBR adheres with varying strengths to different materials, exhibiting the highest adhesion to graphite (SBR@Gr: 7738 ± 781 Nm^{-1}) and quartz glass (SBR@SiO_2: 1963 ± 466 Nm^{-1}) surface. The lowest interfacial strength, by far, occurs between SBR and CMC at just 291 ± 86 Nm^{-1}, which is approximately 37% of the adhesion strength between SBR and copper foil (SBR@Cu: 819 ± 47 Nm^{-1}).

The results of the peel tests can be interpreted considering the surface energy of the involved materials. Adhesion failure is governed by the energy per unit area required to create a new surface and hence induce separation[34]. The low adhesion between SBR and CMC is attributed to the significantly lower surface energies of polymers, typically ranging between 20 mJ/m^2 and 40 mJ/m^2, in comparison to the considerably higher values exhibited by copper (1,360 mJ/m^2), graphite (1,250 mJ/m^2), and quartz glass (980 mJ/m^2)[35,36]. Consequently, a substantially lower peel force is required to remove the SBR film from a CMC surface compared to the other high-energy surfaces analyzed in this study.

Despite the highest surface energy values of copper of all substrates tested, the adhesion of SBR to copper is lower than to graphite and quartz glass. This finding may presumably be ascribed to the porosity of the graphite plate, which allows additional mechanical interlocking of the SBR molecules, resulting in high adhesion values. Whereas, the lower SBR adhesion to copper than to quartz glass may be attributed to possible impurities present on the surface of copper foil and lowering its surface energy[37].

The implementation of these results at the electrode level reveals two key insights. Firstly, adding SBR is essential for ensuring a strong connection between the anode active layer and the current collector, since CMC exhibits even two orders of magnitude lower adhesion to the copper foil (2.3 ± 0.7 Nm^{-1}[18]) compared to SBR. Secondly, given that the interfacial strength between SBR and CMC is significantly inferior to that of the bond between SBR and copper foil, it is highly probable that delamination of the anode layer will occur at the SBR-CMC interface. The data from the existing literature demonstrate that the CMC adsorbs on both graphite[26,27,38] and silicon[30-32] surfaces. Given the poor bonding between CMC and SBR, we postulate that the adsorbed CMC layer on active material particles may act as a barrier, thereby reducing the overall electrode adhesion.

CMC adsorption on active materials

To further investigate the impact of the adsorbed CMC layer on the electrode adhesive strength, measurements were conducted to characterize the CMC adsorption behavior on the AM.

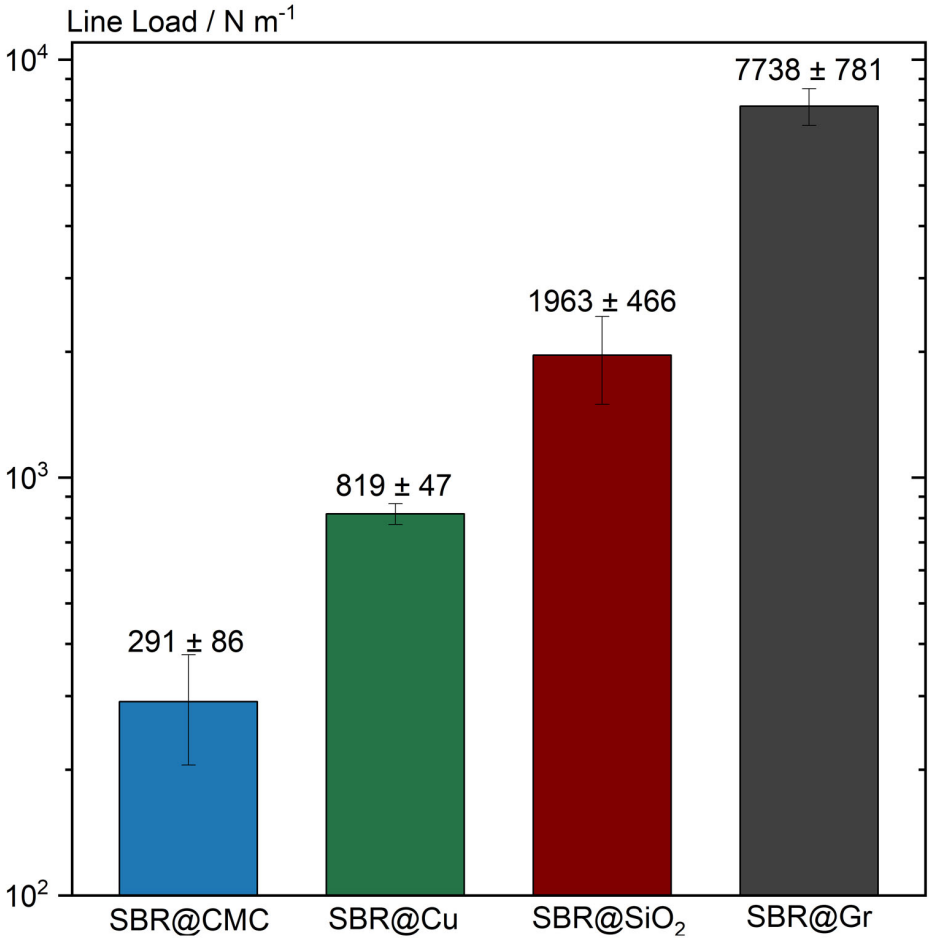

Figure 1. Line load as a measure of adhesion strength for SBR film on CMC film (SBR@CMC), copper foil (SBR@Cu), quartz glass (SBR@SiO_2), and graphite plate (SBR@Gr). Error bars in black represent the standard deviation calculated from measurements with at least three SBR-substrate samples. SBR: Styrene-butadiene rubber; CMC: carboxymethylcellulose.

The polymer adsorption from a solution depends on a multitude of variables, including the concentration and chemical composition of both the polymer and adsorbent, the conformation and M_w of the polymer chains, temperature, or pH and ionic strength[39]. Since the viscosity of a polymer solution is highly sensitive to even slight variations in polymer concentration [Supplementary Figure 2], a rheological approach was employed in order to assess the CMC adsorption capacities of two different silicon materials in comparison to graphite. The active material particles were dispersed in a polymer solution of a known concentration, subjected to centrifugation, and the viscosity of the resulting supernatant was measured in order to determine the concentration of the CMC solution after adsorption. In commercial anodes, CMC with M_w ranging from 150 to 700 kDa is typically utilized. In the present study, the scope of adsorption investigations on active material particles was broadened by extending this range to include CMC with a M_w of 1200 Da to show the influence of this additive more clearly. Industry-relevant silicon-to-CMC volume ratios were investigated. Given the laboratory-scale volumes, the concentration of polymer mother solutions was set at 0.1 vol% (based on water), while the particle concentration was varied. The amount of CMC adsorbed from the solution is expected to increase as more particles are added to the AM/CMC suspension, due to the corresponding rise in the adsorbent's surface area. Consequently, as the R of AM to CMC increases, the viscosity of the supernatants converges towards the viscosity of water. This trend is observed to varying degrees for all active materials investigated in this study [Supplementary Figure 3]. In order to facilitate a

comparison of the adsorption data obtained for particles differing in surface area, the adsorbed volume of CMC was calculated and related to the area of AM, as follows:

$$v_{ads} = \frac{(\varphi_{CMC,0} - \varphi_{CMC}) \cdot V_{solvent}}{S_m \cdot m_{AM}} \quad (1)$$

where v_{ads} represents the specific volume of adsorbed CMC, $\varphi_{CMC,o}$ and φ_{CMC} are volume concentrations of CMC (based on solvent) before and after adsorption, $V_{solvent}$ is the volume of water in CMC solution, and m_{AM} and S_m are mass and specific surface area (BET) of the active material.

Figure 2A-C depicts the specific adsorption volumes of CMC plotted against the *R* of active material to CMC. It should be noted that the adsorption data were obtained in dilute polymer solutions, and thus may not precisely reflect the quantity of CMC adsorbed in a concentrated regime, as would occur in an anode slurry. Nevertheless, as all adsorption experiments were performed in the same polymer concentration regime (dilute), the adsorption capacities of the active materials can be compared. This allows qualitative conclusions to be drawn about the adsorption behavior that would be observed in a concentrated regime.

The adsorbed amount of CMC is shown to be dependent on its M_w, the type of active material, and the particle-to-polymer *R*. All active materials exhibit similar trends in CMC adsorption. First, as *R* increases, the specific amount of adsorbed CMC decreases exponentially, until it reaches a plateau. This outcome was expected as an increase in *R* correlates with an increased surface area of the adsorbent. Consequently, while the total amount of adsorbed CMC grows, the polymer density on the surface area decreases. The second trend observed is that an increase in CMC M_w correlates with a greater amount of adsorbed polymer, which was anticipated since a monolayer of absorbed molecules has a higher mass at a higher M_w. Furthermore, the results indicate that CMC exhibits a greater affinity for the micro-Si surface than for graphite. This can be attributed to the variations in surface properties of the active materials, which have a predominant influence on the adsorption mechanism and, consequently, on the quantity of adsorbed polymer. The CMC adsorption on graphite is due to the hydrophobic attraction between the cyclic structure of CMC and the hydrophobic graphite basal planes[27,40]. However, on a silicon surface covered by a partially hydrolyzed native silicon oxide layer[41], adsorption can occur through either covalent or hydrogen bonding, depending on the pH[28,42,43]. This process occurs via the interaction of the carboxyl groups of the CMC and the silanol groups present on the silicon surface.

Interestingly, while CMC exhibits the strongest affinity for micro-Si among all the materials studied, its interaction with nano-Si is notably poor, irrespective of the CMC M_w and *R*. The additional thermogravimetric analysis (TGA) [Supplementary Figure 4] of the powders reveals a greater mass loss of the nano-Si sample compared to micro-Si, which may be attributed to the presence of a greater quantity of surface modifiers on the nano-Si particles. Further confirmation of the differences in surface properties of the silicon powders could be obtained through zeta potential measurements [Supplementary Figure 5]. The zeta potential of both materials displays the typical trend characteristic of silicon powders. The oxidized silicon surface undergoes hydrolysis in water, forming silanol (SiOH) groups[44]. As the pH rises, the SiOH groups on the silicon surface undergo deprotonation, resulting in a surface dominated by SiO^-, causing the zeta potential to decrease. However, in aqueous media with a pH below 4, the SiOH groups interact with H^+, forming $SiOH_2^+$, which leads to an increase in zeta potential[39]. The overall higher zeta potential of nano-Si can be ascribed to the lower number of SiOH groups. Since these sites function as centers for CMC adsorption[45], their reduced quantity may result in significantly lower polymer adsorption.

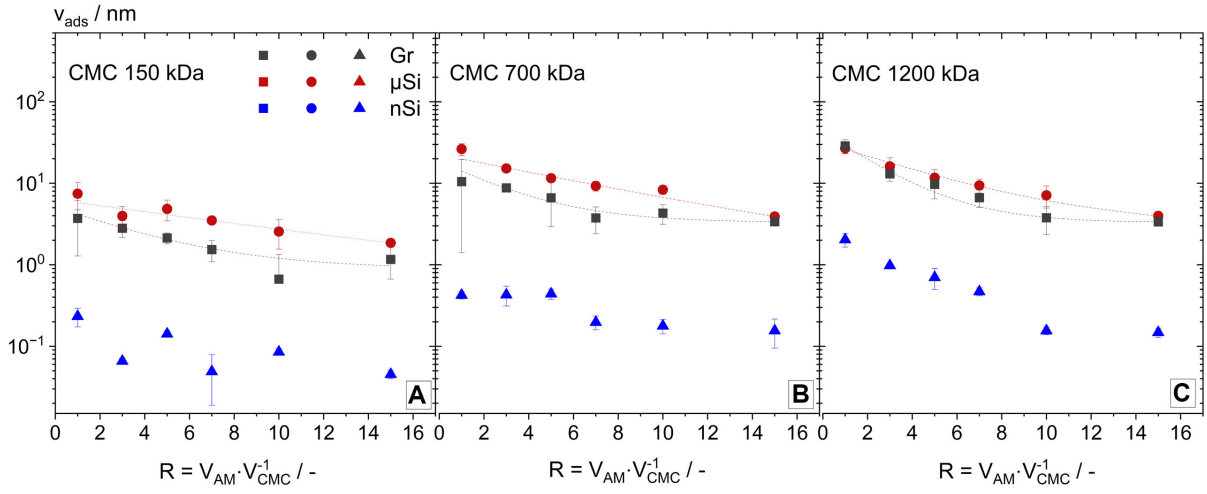

Figure 2. Adsorbed amounts of CMC of 150 kDa (A), 700 kDa (B), and 1200 kDa (C) on three anode active materials: graphite (Gr), micro- (μSi) and nano- (nSi) silicon as a function of the volume ratio *R* of active material to CMC. Error bars represent the standard deviation calculated from measurements with at least three supernatant samples of one formulation. CMC: Carboxymethylcellulose.

We did not consider the adsorption of CMC on CB here, since the fraction of CB is much smaller than that of the active materials and hence does not contribute significantly to the adhesion of anode layers to the current collector.

Adhesion of anodes

The active anode layer is bonded to the copper current collector via polymeric binders. A series of negative electrode samples were produced and subjected to a 90°-peel test to investigate how the adhesion between SBR and three potential attachment surfaces on the electrode active layer side (active material particles, CB, and CMC) affects the adhesive strength between the anode layer and copper current collector. While the peel area in macroscopic adhesion experiments (as described in the Results and Discussion section, "Adhesion of SBR films to anode components") is larger than the particle/particle or particle/current collector contact area in electrodes, the surface energy governing adhesion failure remains a material constant. Therefore, the findings from macroscopic adhesion experiments can be applied to point-like adhesion present in electrodes.

As illustrated in Figure 3, the line load of the graphite anodes exhibits a decline with an increase in CMC M_w. Given that higher M_w corresponds to a greater uptake of CMC onto the particle surface, as demonstrated in Figure 2, the adsorbed CMC layer may act as a barrier, inhibiting direct and significantly stronger SBR-particle bonding, thereby reducing the overall adhesion of the anode layer to the current collector. To verify this hypothesis, graphite electrodes with a non-adsorbing PEO binder[46] were fabricated, both with and without the addition of SBR. In contrast to anodes with CMC, the use of PEO ensures that graphite particles are free from adsorbed polymeric thickener layers, thereby eliminating its negative effect on anode adhesion. Consequently, the line load of the PEO anodes [Supplementary Figure 6] is approximately twice as high as the adhesive force of the graphite anodes with adsorbing CMC and the same concentration of SBR. As PEO does not contribute to the adhesion strength of the anodes [Supplementary Figure 6], it becomes evident that when SBR can directly dock to the active particle surface, the adhesion strength significantly increases. Nevertheless, even with a non-adsorbing thickener ensuring direct contact between SBR molecules and particles, the measured line loads are found to be significantly lower than those observed between bulk materials [Figure 1]. This discrepancy is attributed to the higher contact surface area

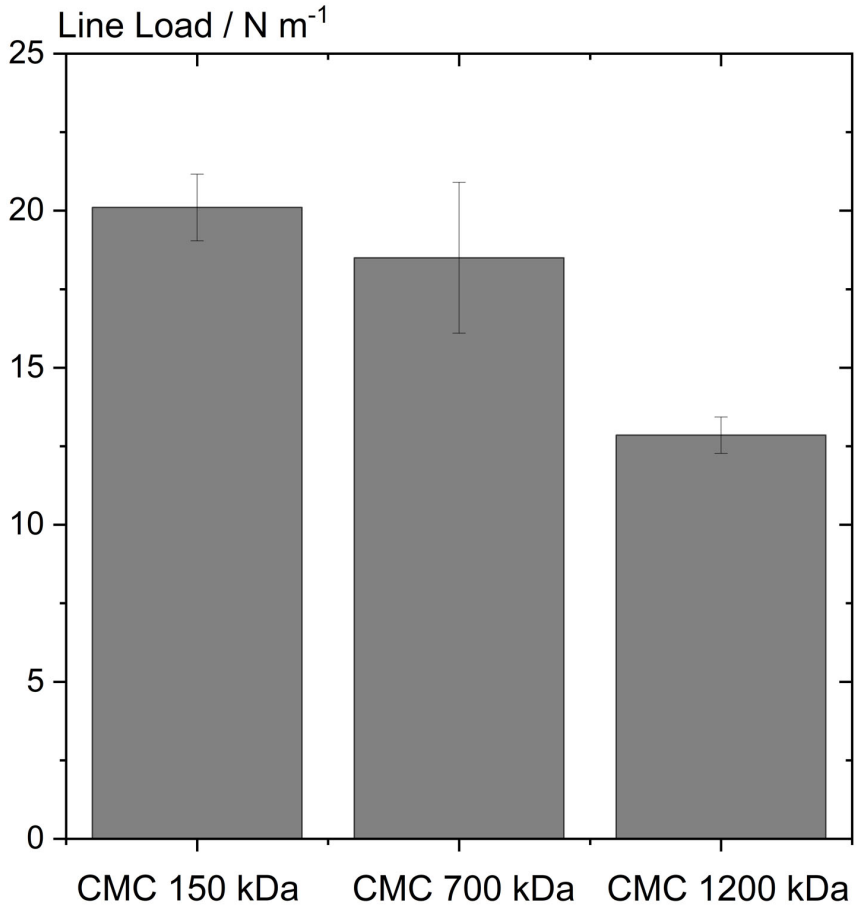

Figure 3. Line loads of graphite anodes prepared with CMC of varying molecular weights of 150 kDa, 700 kDa and 1200 kDa. Error bars represent the standard deviation calculated from measurements with at least ten electrode samples. CMC: Carboxymethylcellulose.

between SBR films and substrates in comparison to a single-point interface between anode components, which is a characteristic of SBR as a point-to-surface contact binder[47].

Thus, the line load can be considered as a function of the amount of polymeric thickener adsorbed on the particle surface. This correlation is depicted for graphite and graphite-silicon composite anodes in Figure 4. In composite anodes, 20 wt% of graphite was substituted with micro-Si or nano-Si, and the active material to polymer R was 39 and 7 for graphite and silicon, respectively. The adsorbed polymer amount refers to the amount of polymer (CMC or PEO) adsorbed on graphite or silicon active material, and it varies due to CMC M_w. Graphite anodes with non-adsorbing PEO demonstrate the highest adhesion to the copper foil. In the case of anodes comprising an adsorbing polymeric thickener, it was found that the adhesion strength declines with increasing amount of adsorbed polymer. This suggests that the likelihood of SBR directly adhering to active material particles is reduced when a greater quantity of polymer is adsorbed. As the SBR-CMC bond is the weakest, as demonstrated in the Results and Discussion section, "Adhesion of SBR films to anode components", it can be concluded that the electrode adhesion to the copper foil is directly affected by the adsorbed CMC layer.

Notably, the line load of nano-Si-graphite anodes is significantly reduced compared to the other investigated electrodes, although the CMC adsorption on nano-Si is more than an order of magnitude lower

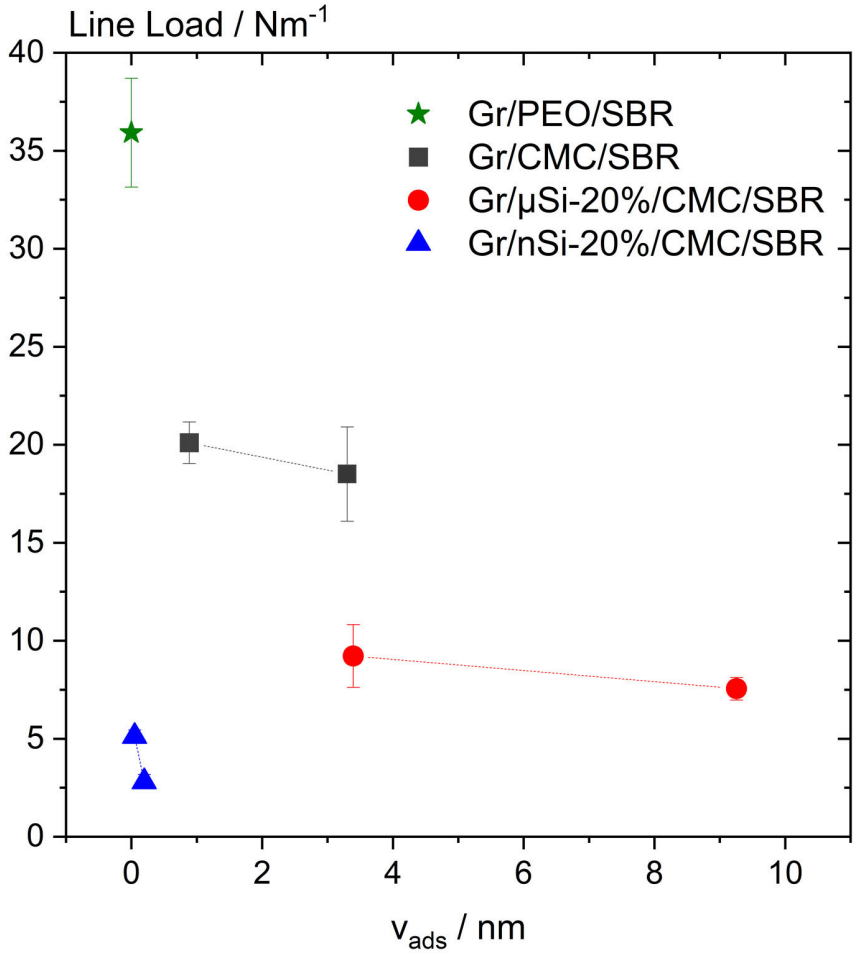

Figure 4. Line loads of graphite and graphite-silicon anodes prepared with CMC/SBR or PEO/SBR binder system as a function of specific volume of adsorbed polymeric thickener (CMC or PEO). The adsorbed polymer amount refers to the data obtained from the adsorption measurements conducted with particles dispersed in a dilute polymer solution [Figure 2]. Error bars represent the standard deviation calculated from measurements with at least ten electrode samples. SBR: Styrene-butadiene rubber; CMC: carboxymethylcellulose; PEO: polyethylene oxide.

than on graphite or micro-Si. This phenomenon can be attributed to structural effects. In an aqueous environment, silicon nanoparticles tend to agglomerate. The diameter of these agglomerates ranges from 0.77 µm ($x_{10,3}$) to 22 µm ($x_{90,3}$) with an average value of 5.55 µm ($x_{50,3}$). SBR molecules with a diameter of up to 170 nm are capable of diffusing into the porous structure of these nano-Si agglomerates [Figure 5A and B] and becoming trapped. As a result, a markedly reduced amount of SBR is able to come into contact with the copper interface and bond the particles to the current collector foil, thereby reducing the overall adhesion strength of the electrode. This hypothesis could be confirmed through a simple experimental procedure involving the preparation of a nano-Si/water/SBR suspension, followed by centrifugation. Subsequently, the mass increase of the dry sediment due to the oxidation of the silicon surface, and the remaining SBR within the silicon agglomerates was determined. The results demonstrated that 40.3 ± 7.3% of the initial quantity of SBR was trapped in the nano-Si sediment. For comparison, the same experiment was conducted with micro-Si particles, which yielded a considerably lower percentage of the initial SBR quantity of 9.1 ± 3.6% remaining in the sediment. These findings indicate that while using nanoparticles as an active material, electrode adhesion is influenced by both thickener adsorption and the structural effect described above. The latter leads to a reduction in the overall amount of SBR available to

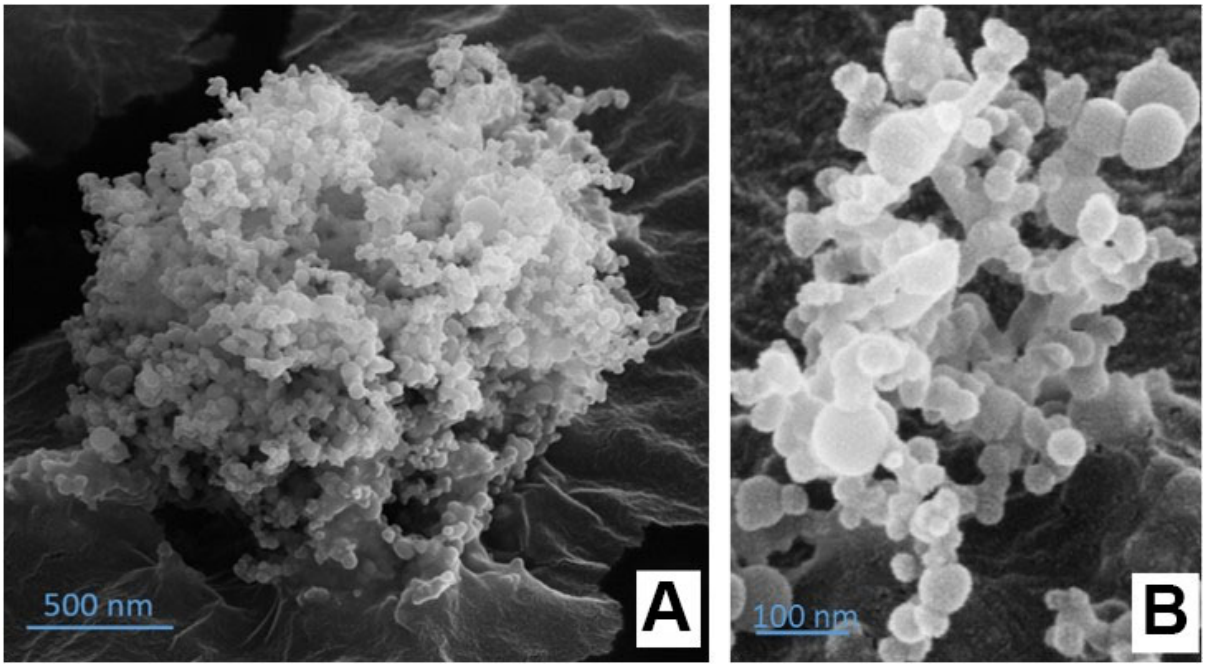

Figure 5. SEM images of a nano-Si agglomerate at magnifications 100,000x (A) and 200,000x (B) (Zeiss Leo 1530, 10 kV). SEM: scanning electron microscope.

bond with the copper foil, thus exerting a pronounced negative impact on the anode adhesion.

CONCLUSIONS

In summary, the present study investigates how the adsorption of CMC on active material particles exerts a negative impact on the adhesion of graphite and graphite-silicon anodes, despite the fact that, in the absence of SBR, it does not affect electrode adhesion and is added to the anode slurries as a thickener and stabilizer. As SBR represents the component of the slurry responsible for maintaining the robust connection between the copper current collector and the anode layer constituents (active material particles, CB, CMC), we conducted 90°-peel tests to ascertain the adhesion strength between the SBR films and the individual anode components. The results demonstrate that the highest interfacial strength is observed between SBR and graphite, followed by adhesion between SBR and quartz glass (served as an equivalent surface for the silicon active material). The weakest bonding occurs between SBR and CMC, and given that this adhesion value is significantly lower than the adhesion between SBR and copper foil, delamination of the anode active layer from the copper current collector will occur most probably at the SBR-CMC interface. Therefore, we proposed that the adsorbed CMC layer may act as a barrier, impeding the strong adhesion of the active material particles to the copper foil. Furthermore, the CMC adsorption behavior was determined as a function of molecular mass for three different AMs: graphite, micro- and nano-silicon. The results indicate that CMC exhibits the highest affinity for the micro-silicon surface, followed by graphite, and the lowest affinity for the nano-silicon. In the last section, we demonstrate how the adhesion between the SBR and individual anode components is reflected in the complex polymer/particle system that constitutes the anode. An increase in CMC M_w, corresponding to greater uptake of the polymer on the active material surface, has been observed to result in a decline in the line load of the graphite and graphite-micro-Si composite anodes. Moreover, the utilization of a non-adsorbing polymer as a thickener has been shown to significantly enhance the adhesion of the graphite anode, which can be attributed to the direct interconnection between the particle and the SBR polymer. In addition, the adhesion of electrodes can be

affected by the structure of the active materials. We showed that SBR particles can diffuse inside nano-silicon agglomerates and become trapped. Consequently, graphite-nano-silicon composite anodes exhibit markedly low adhesion even though the nano-silicon particles adsorb only a very low amount of CMC.

As demonstrated in our previous research[17], sufficiently high adhesion of the anodes is crucial for their manufacturing process. At the same time, considering that high SBR content impedes electrochemical cell performance and reduces cyclic stability, high adhesion and cohesion with low SBR amount is desired to improve LIB quality and lifespan. This can be achieved by implementing the findings of the present study. For optimizing a commercial CMC/SBR binder system, choosing appropriate CMC grades with lower M_w or DS to reduce adsorption can enhance the mechanical performance of anodes.

Moreover, other potential strategies to mitigate the negative effects of binder adsorption on anode adhesion can include surface modifications of active material particles to ensure particle stabilization without thickener adsorption, or the use of binders with strong thickening properties but minimal or no adsorption on active material particles. The investigation of the latter approach is the focus of our ongoing research.

DECLARATIONS

Acknowledgments

We thank Elkem and ChemPoint for supplying the micron-sized silicon material and CMCs, respectively. Special thanks go to Doménica Estefanía Paz Puga, Thomas Textor, Christina Eichenseher for their experimental assistance and Birgit Huber for TGA measurements.

Authors' contributions

Conceptualization, data curation, formal analysis, investigation, methodology, project administration, validation, visualization, writing - original draft, writing - review and editing: Hofmann, K.

Conceptualization, funding acquisition, resources, supervision, writing -review and editing: Willenbacher, N.

Availability of data and materials

The data supporting the findings of this study are available within this Article and its Supplementary Materials. Further data are available from the corresponding author upon request.

Financial support and sponsorship

This work was supported by the German Research Foundation, grant no. WI 3138/33-1.

Conflicts of interest

All authors declared that there are no conflicts of interest.

Ethical approval and consent to participate

Not applicable.

Consent for publication

Not applicable.

REFERENCES

1. International Energy Agency (IEA), Paris, Global EV outlook 2024. Available from: https://www.iea.org/reports/global-ev-outlook-2024. [Last accessed on 14 Apr 2025].
2. Miao, Y.; Hynan, P.; von, J. A.; Yokochi, A. Current Li-ion battery technologies in electric vehicles and opportunities for advancements. *Energies* **2019**, *12*, 1074. DOI
3. Cholewinski, A.; Si, P.; Uceda, M.; Pope, M.; Zhao, B. Polymer binders: characterization and development toward aqueous electrode fabrication for sustainability. *Polymers* **2021**, *13*, 631. DOI PubMed PMC
4. Liu, Y.; Zhang, R.; Wang, J.; Wang, Y. Current and future lithium-ion battery manufacturing. *iScience* **2021**, *24*, 102332. DOI PubMed PMC
5. Lestriez, B. Functions of polymers in composite electrodes of lithium ion batteries. *C. R. Chim.* **2010**, *13*, 1341-50. DOI
6. Lopez, C. G.; Rogers, S. E.; Colby, R. H.; Graham, P.; Cabral, J. T. Structure of sodium carboxymethyl cellulose aqueous solutions: a SANS and rheology study. *J. Polym. Sci. B. Polym. Phys.* **2015**, *53*, 492-501. DOI PubMed PMC
7. Lopez, C. G.; Colby, R. H.; Cabral, J. T. Electrostatic and hydrophobic interactions in NaCMC aqueous solutions: effect of degree of substitution. *Macromolecules* **2018**, *51*, 3165-75. DOI
8. Lee, J.; Paik, U.; Hackley, V. A.; Choi, Y. Effect of carboxymethyl cellulose on aqueous processing of natural graphite negative electrodes and their electrochemical performance for lithium batteries. *J. Electrochem. Soc.* **2005**, *152*, A1763. DOI
9. Lim, S.; Ahn, K. H.; Yamamura, M. Latex migration in battery slurries during drying. *Langmuir* **2013**, *29*, 8233-44. DOI PubMed
10. Gordon, R.; Orias, R.; Willenbacher, N. Effect of carboxymethyl cellulose on the flow behavior of lithium-ion battery anode slurries and the electrical as well as mechanical properties of corresponding dry layers. *J. Mater. Sci.* **2020**, *55*, 15867-81. DOI
11. Jaiser, S.; Kumberg, J.; Klaver, J.; et al. Microstructure formation of lithium-ion battery electrodes during drying - an ex-situ study using cryogenic broad ion beam slope-cutting and scanning electron microscopy (Cryo-BIB-SEM). *J. Power. Sources.* **2017**, *345*, 97-107. DOI
12. Jaiser, S.; Müller, M.; Baunach, M.; Bauer, W.; Scharfer, P.; Schabel, W. Investigation of film solidification and binder migration during drying of Li-ion battery anodes. *J. Power. Sources.* **2016**, *318*, 210-9. DOI
13. Westphal, B. G.; Kwade, A. Critical electrode properties and drying conditions causing component segregation in graphitic anodes for lithium-ion batteries. *J. Energy. Storage.* **2018**, *18*, 509-17. DOI
14. Chen, H.; Ling, M.; Hencz, L.; et al. Exploring chemical, mechanical, and electrical functionalities of binders for advanced energy-storage devices. *Chem. Rev.* **2018**, *118*, 8936-82. DOI
15. Petrie, E. *Adhesive bonding of textiles: principles, types of adhesive and methods of use.* In: *Joining Textiles Principles and Applications*; Woodhead Publishing Series in Textiles; Elsevier, 2013; pp. 225-74. DOI
16. Mcbain, J. W.; Hopkins, D. G. On adhesives and adhesive action. *J. Phys. Chem.* **1925**, *29*, 188-204. DOI
17. Hofmann, K.; Hegde, A. D.; Liu-theato, X.; Gordon, R.; Smith, A.; Willenbacher, N. Effect of mechanical properties on processing behavior and electrochemical performance of aqueous processed graphite anodes for lithium-ion batteries. *J. Power. Sources.* **2024**, *593*, 233996. DOI
18. Choi, S.; Kwon, T. W.; Coskun, A.; Choi, J. W. Highly elastic binders integrating polyrotaxanes for silicon microparticle anodes in lithium ion batteries. *Science* **2017**, *357*, 279-83. DOI
19. Ye, R.; Liu, J.; Tian, J.; et al. Novel binder with cross-linking reconfiguration functionality for silicon anodes of lithium-ion batteries. *ACS. Appl. Mater. Interfaces.* **2024**, *16*, 16820-9. DOI
20. Yu, Y.; Yang, C.; Jiang, Y.; Zhu, J.; Zhang, J.; Jiang, M. Consecutive covalent bonds reconstruct robust dual-interfaces by carbonized binder to enable conductive-additive-free durable silicon anode. *Nano. Energy.* **2024**, *130*, 110108. DOI
21. Ren, W. F.; Le, J. B.; Li, J. T.; et al. Improving the electrochemical property of silicon anodes through hydrogen-bonding cross-linked thiourea-based polymeric binders. *ACS. Appl. Mater. Interfaces.* **2021**, *13*, 639-49. DOI
22. Xiang, Y.; Xu, H.; Deng, J.; Li, J.; Nazir, M. A.; Bao, S. Spiderweb-like three-dimensional cross-linked AGE binder for high performance silicon-based lithium battery. *ACS. Appl. Energy. Mater.* **2025**, *8*, 2973-81. DOI
23. Kumberg, J.; Bauer, W.; Schmatz, J.; et al. Reduced drying time of anodes for lithium-ion batteries through simultaneous multilayer coating. *Energy. Tech.* **2021**, *9*, 2100367. DOI
24. Bak, C.; Kim, K.; Lee, H.; et al. Advanced multilayer model electrode for binder distribution within composite electrodes of lithium batteries. *Chem. Eng. J.* **2024**, *483*, 148913. DOI
25. Burger, D.; Keim, N.; Shabbir, J.; et al. Simultaneous primer coating for fast drying of battery electrodes. *Energy. Tech.* **2025**, *13*, 2401668. DOI
26. Lee, J.; Paik, U.; Hackley, V. A.; Choi, Y. Effect of poly(acrylic acid) on adhesion strength and electrochemical performance of natural graphite negative electrode for lithium-ion batteries. *J. Power. Sources.* **2006**, *161*, 612-6. DOI
27. Mori, T.; Kitamura, K. Effect of adsorption behaviour of polyelectrolytes on fluidity and packing ability of aqueous graphite slurries. *Adv. Powder. Technol.* **2017**, *28*, 280-7. DOI
28. Bridel, J.; Azaïs, T.; Morcrette, M.; Tarascon, J.; Larcher, D. In situ observation and long-term reactivity of Si/C/CMC composites electrodes for Li-ion batteries. *J. Electrochem. Soc.* **2011**, *158*, A750-9. DOI
29. Huang, L.; Chen, D.; Li, C.; Chang, Y.; Lee, J. Dispersion homogeneity and electrochemical performance of Si anodes with the addition of various water-based binders. *J. Electrochem. Soc.* **2018**, *165*, A2239-46. DOI
30. Kim, K. J.; Ahn, K. H. Effects of sodium carboxymethyl cellulose and poly (acrylic acid) on the agglomeration behavior of aqueous

silicon suspensions. *Colloids. Surf. A. Physicochem. Eng. Asp.* **2023**, *673*, 131801. DOI

31. Park, J. H.; Ahn, C. H.; Ahn, K. H. Rheological behavior and microstructure formation of Si/C anode slurries for Li-ion batteries. *Korea-Aust. Rheol. J.* **2023**, *35*, 335-47. DOI
32. Kim, B.; Song, Y.; Youn, B.; Lee, D. Dispersion homogeneity of silicon anode slurries with various binders for Li-ion battery anode coating. *Polymers* **2023**, *15*, 1152. DOI PubMed PMC
33. Haberzettl, P.; Filipovic, N.; Vrankovic, D.; Willenbacher, N. Processing of aqueous graphite-silicon oxide slurries and its impact on rheology, coating behavior, microstructure, and cell performance. *Batteries* **2023**, *9*, 581. DOI
34. Andrews, E. H.; Kinloch, A. J. Mechanics of adhesive failure. I. *Proc. R. Soc. Lond. A.* **1973**, *332*, 385-99. DOI
35. Kinloch, A. J. *Adhesion and adhesives: science and technology*, 1th ed.; Springer Science & Business Media, 2087. DOI
36. Y.K. Surface energy of crystalline and vitreous silica. *Glass. Ceram.* **2000**, *57*, 374-7. DOI
37. Murdock, A. T.; van, E. C. D.; Britton, J.; et al. Targeted removal of copper foil surface impurities for improved synthesis of CVD graphene. *Carbon* **2017**, *122*, 207-16. DOI
38. Chang, W. J.; Lee, G. H.; Cheon, Y. J.; et al. Direct observation of carboxymethyl cellulose and styrene-butadiene rubber binder distribution in practical graphite anodes for Li-ion batteries. *ACS. Appl. Mater. Interfaces.* **2019**, *11*, 41330-7. DOI
39. Burdette-trofimov, M. K.; Armstrong, B. L.; Rogers, A. M.; et al. Understanding binder-silicon interactions during slurry processing. *J. Phys. Chem. C.* **2020**, *124*, 13479-94. DOI
40. Kwon, T. W.; Choi, J. W.; Coskun, A. The emerging era of supramolecular polymeric binders in silicon anodes. *Chem. Soc. Rev.* **2018**, *47*, 2145-64. DOI PubMed
41. Lee, Y. M.; Lee, J. Y.; Shim, H.; Lee, J. K.; Park, J. SEI layer formation on amorphous Si Thin electrode during precycling. *J. Electrochem. Soc.* **2007**, *154*, A515. DOI
42. Hochgatterer, N. S.; Schweiger, M. R.; Koller, S.; et al. Silicon/graphite composite electrodes for high-capacity anodes: influence of binder chemistry on cycling stability. *Electrochem. Solid-State. Lett.* **2008**, *11*, A76. DOI
43. Mazouzi, D.; Lestriez, B.; Roué, L.; Guyomard, D. Silicon composite electrode with high capacity and long cycle life. *Electrochem. Solid-State. Lett.* **2009**, *12*, A215. DOI
44. Zhang, Q.; Li, W.; Gu, M.; Jin, Y. Dispersion and rheological properties of concentrated silicon aqueous suspension. *Powder. Technol.* **2006**, *161*, 130-4. DOI
45. Vogl, U. S.; Das, P. K.; Weber, A. Z.; Winter, M.; Kostecki, R.; Lux, S. F. Mechanism of interactions between CMC binder and Si single crystal facets. *Langmuir* **2014**, *30*, 10299-307. DOI PubMed
46. Bitsch, B. Verwendung von kapillarsuspensionen zur prozessierung von lithium-ionen batterieelektroden. Ph.D. Dissertation, Karlsruher Institut für Technologie (KIT), Karlsruhe,Germany, 2017. Available from: https://publikationen.bibliothek.kit.edu/1000064637. [Last accessed on 15 Apr 2025]
47. Salini, P. S.; Gopinadh, S. V.; Kalpakasseri, A.; John, B.; Thelakkattu, D. M. Toward greener and sustainable Li-ion cells: an overview of aqueous-based binder systems. *ACS. Sustain. Chem. Eng.* **2020**, *8*, 4003-25. DOI